Use of Lambert's Theorem for the n–Dimensional Coulomb Problem

Vassiliki Kanellopoulos,[1,2,*] Manfred Kleber,[1] and Tobias Kramer[3,4]

[1] *Physik Department T30, Technische Universität München James-Franck-Str., 85747 Garching, Germany.*
[2] *Laboratory of Atomic and Solid State Physics, Cornell University, Ithaca, NY 14853, USA*
[3] *Institute for Theoretical Physics, Universität Regensburg, 93040 Regensburg, Germany.*
[4] *Department of Physics, Harvard University, 17 Oxford Street, Cambridge, MA 02138, USA.*

(Dated: April 21, 2009)

We present the analytical solution in closed form for the semiclassical limit of the quantum mechanical Coulomb Green function in position space in n dimensions. We utilize a projection method which has its roots in Lambert's theorem and which allows us to treat the system as an essentially one dimensional problem. The semiclassical result assumes a simple analytical form and is well suited for a numerical evaluation. The method can also be extended to classically forbidden space regions. Already for moderately large principal quantum numbers $\nu \geq 5$, the semiclassical Green function is found to be an excellent approximation to the quantum mechanical Green function.

PACS numbers: 03.65.Sq,03.65.Ge,03.65.Nk

I. INTRODUCTION

The laws of planetary motion remained for a long time a mind–puzzling challenge. It was Johannes Kepler who published 400 years ago his book *Astronomia Nova* which contained his famous first two laws on planetary motion. Kepler's conclusion that all planets move in elliptical orbits with the Sun in one focus was based on his ingenious evaluation of very accurate observations of the path of the planet Mars by the astronomer Tycho Brahe, the last of many important astronomers who made their observations without the help of a telescope. As is well known, the mathematical construction scheme for expressing the motion of bodies in a gravitational $(1/r)$ potential in mathematical terms goes back to the days of Newton's *Principia Mathematica*, first published in 1687. This work unifies Galileo's ideas about motion in a gravitational field and Kepler's laws on planetary motion.
In the 18^{th} century it was still a major problem to follow the motion of a planet along its elliptical path or, more general, along a curved trajectory. For the $1/r$–potential this difficulty was solved by the Swiss Mathematician and Physicist Johann Heinrich Lambert who proved geometrically that the transfer time along a planetary orbit connecting two position vectors $\mathbf{r}$ and $\mathbf{r}'$ depends only on the two combinations α_+ and α_-,

$$\alpha_+ = r + r' + s \;\text{ and }\; \alpha_- = r + r' - s \,, \qquad (1)$$

where s is the distance between $\mathbf{r}$ and $\mathbf{r}'$. The position vectors are meant relative to the force center (in Lambert's case the Sun). The additional dependence of the travel time on E will be discussed later. Equation (1) is a peculiarity of the $1/r$–potential. The fact that the transfer time depends only on α_+ and α_- is called Lambert's theorem.

The agreement between the calculated and observed positions of the planets was historically the most important success of classical physics. With the advent of quantum mechanics, the Kepler problem was replaced by the Coulomb problem for the hydrogen atom. Feynman's path integral method revealed the close connection between classical and quantum mechanics. The fixed–energy propagator for the Coulomb problem is known analytically both in configuration and momentum space [1, 2, 3, 4, 5, 6, 7, 8, 9]. However the corresponding semiclassical approximation has not been given before in closed analytic form because of the appearance of a rather complicated prefactor, the so called Van Vleck–Pauli–Morette determinant. The semiclassical approach to the Coulomb problem in $n > 1$ dimensions the determinant has been calculated so far only numerically [10]. Based on Lambert's theorem, we will derive a simple and useful analytic expression for the Van Vleck–Pauli–Morette determinant in n spatial dimensions. The result will put us in the position to derive a two-line expression for the semiclassical Green function.

II. LAMBERT'S THEOREM FOR THE REDUCED ACTION

It is a simple exercise in classical mechanics to analyze the relative motion for the Kepler or Coulomb Hamiltonian

$$H = \frac{\mathbf{p}^2}{2\mu} - \frac{K_c}{r} \,, \qquad (2)$$

where μ is the reduced mass and K_c the strength of the attractive $1/r$ potential. The corresponding motion in time is given by

$$t - t' = \sqrt{\frac{\mu a}{K_c}} \int_{r'}^{r} \frac{\tilde{r}}{\sqrt{2a\tilde{r} - \tilde{r}^2 - a\Lambda^2/(\mu K_c)}} \, \mathrm{d}\tilde{r} \,. \qquad (3)$$

Here $\Lambda = \mu r^2 \dot{\phi}$ is the angular momentum about the center of force for elliptic motion with semimajor axis

*Currently Marie Curie Fellow at CERN on the PARTNER ITN, PITN-GA-2008-215840

$a = K_c/(2|E|)$, for $E < 0$.
An important element for the transition from classical mechanics to quantum mechanics is the reduced action W, also called action integral S. In order to avoid confusion, we reserve S here for Hamilton's principal function (see below). Within the time–independent Hamilton–Jacobi theory the reduced action W is given by

$$W(\mathbf{r}, \mathbf{r}'; E) = \int_{\mathbf{r}'}^{\mathbf{r}} \mathbf{p}(\tilde{\mathbf{r}}) \cdot \mathrm{d}\tilde{\mathbf{r}} \,. \tag{4}$$

For elliptic motion in the x–y–plane an explicit evaluation of Eq. (4) is easily achieved by introducing for example Cartesian coordinates with the origin at the center of the ellipse

$$x = a\cos\xi \,, \quad y = b\sin\xi \,, \tag{5}$$

where $b = a\sqrt{1-\epsilon^2}$ is the semiminor axis of the Kepler ellipse with eccentricity ϵ. If we substitute Eq. (5) into Eq. (4) and use

$$t - t' = \sqrt{\frac{\mu a^3}{K_c}}(\xi - \epsilon\sin\xi - \xi' + \epsilon\sin\xi') \tag{6}$$

for the transfer time between two points on the ellipse, we obtain

$$W(\mathbf{r}, \mathbf{r}'; E) = \sqrt{\mu a K_c}\,(\xi + \epsilon\sin\xi - \xi' - \epsilon\sin\xi'). \tag{7}$$

$W(\mathbf{r}, \mathbf{r}'; E)$ is a function of E and of the initial and final coordinates $\mathbf{r}$ and $\mathbf{r}'$ of the planet. Therefore other dynamical quantities, like the orbital angular momentum Λ must be eliminated. Hence we have to get rid of $\epsilon = \sqrt{1 - 2|E|\Lambda^2/(\mu K_c^2)}$ in Eq. (7). A few algebraic manipulations (see App. A) lead to

$$W(\mathbf{r}, \mathbf{r}'; E) = \sqrt{\mu a K_c}\,(\gamma + \sin\gamma - \delta - \sin\delta) \tag{8}$$

with

$$\sin^2\frac{\gamma}{2} = \frac{r + r' + s}{4a} \quad \text{and} \quad \sin^2\frac{\delta}{2} = \frac{r + r' - s}{4a} \,. \tag{9}$$

In the last equation and in what follows r and r' are the distances from the focus of the ellipse (i. e. the center of force) to two arbitrary points on the elliptical orbit. As before s stands for the distance between r and r'. The situation is depicted in Fig. 1. It was Lambert [11] who succeeded to map elliptical motion to collinear motion. He also proved ([11], Lemma 24) that for fixed energy $E < 0$, the classically allowed elliptic motion from a given initial point N to a final point M can generally occur on two different ellipses unless we have circular motion (compare [4], p. 27). From the last two equations it becomes obvious that the reduced action W is a function of $\alpha_+ = r + r' + s$ and $\alpha_- = r + r' - s$. Note that the energy dependence of W enters through the semimajor axis $a = K_c/(2|E|)$.
Another piece of information is Hamilton's principal function $S(\mathbf{r}, \mathbf{r}', \tau)$ which follows from the well–known Legendre transformation

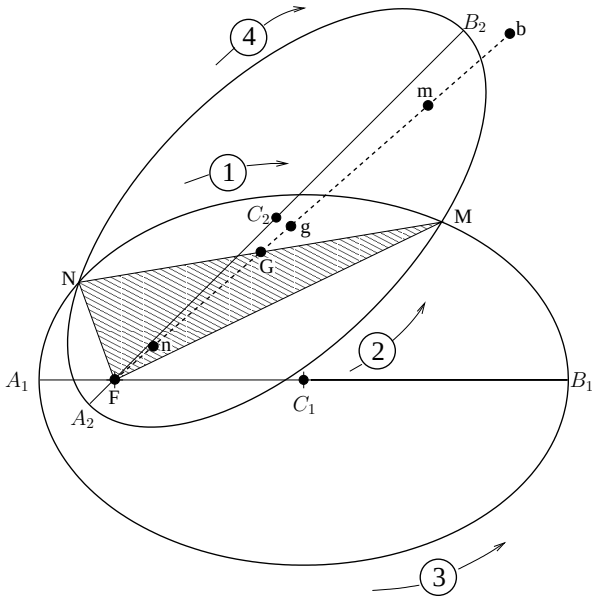

FIG. 1: Lambert's projection of elliptic motion to collinear motion. Shown are two ellipses with the same lengths of the semimajor axes $\frac{1}{2}A_1B_1 = \frac{1}{2}A_2B_2$ and a common focus located at F. The centers of the two ellipses are denoted by C_1 and C_2. Lambert's lemma 24 allows to relate the motion from N to M on both ellipses to a common collinear motion on the degenerate linear ellipse Fb, where the points n and m are chosen such that the time of flight (TOF) along nm equals the TOF along the elliptical arc NM on the first ellipse. On the second ellipse the TOF along the arc NB_2M equals the TOF along nbm. The points n and m are found by marking the point G halfway between N and M. Then the major axis $Fb = A_1B_1 = A_2B_2$ of the linear ellipse is drawn starting at F and running through G. On this line the point g is placed at the distance $Fg = \frac{1}{2}(FN + FM)$. Finally n and m are given by the intersection points of a circle around g with radius $GN = GM$. This construction shows that the sum of the lengths of the shaded triangle $\alpha_\pm = FN + FM \pm NM$ is equal to $\alpha_\pm = Fn + Fm \pm nm$. The ficticious collinear motion goes back to Lambert and can be picturized as the limit of an elliptic motion with extremely small semiminor axis b. The eccentricity approaches one from below in such a way that the moving particle turns around at F with very high but of course still non-relativistic velocity.

$$S(\mathbf{r}, \mathbf{r}', \tau) = W(\mathbf{r}, \mathbf{r}', E) - E\tau \,. \tag{10}$$

The travel time $\tau = t - t'$ from $\mathbf{r}'$ to $\mathbf{r}$ can be calculated from

$$\tau = \frac{\partial W}{\partial E} \,, \tag{11}$$

or directly from Eq. (6) by using the method of App. A. The result is

$$\tau = t - t' = \sqrt{\frac{\mu a^3}{K_c}}(\gamma - \sin\gamma - \delta + \sin\delta) \,. \tag{12}$$

Equation (12) is Lambert's theorem ([11], p. 102) for the travel time between N and M. In our case it is more important to point out that Lambert's theorem is not only valid for the travel time but also for the reduced action W and, although not of importance here, for Hamilton's principal function S. With these results in mind, we are now in a position to calculate the semiclassical Green function.

III. COULOMB TRAJECTORIES AND LAMBERT'S THEOREM

In quantum physics, the Kepler problem becomes the Coulomb problem. The connection between classical and quantum mechanics is conveniently established through the introduction of the quantum mechanical Green function, also called propagator. The Green function is the mathematical vehicle that allows a particle to go from an initial configuration to a final one. In configuration space it represents the transition amplitude to travel from $\mathbf{r}'$ to $\mathbf{r}$. Each classical trajectory in Fig. 1 has sharp energy and travel time. In quantum mechanics the travel may occur either with fixed energy or in a given time. Travel with fixed energy is characterized by the nonrelativistic energy Coulomb Green function which was obtained by Hostler [12] in configuration space in closed form, starting from a partial-wave expansion. The Coulomb Green function in momentum space was derived soon after by Schwinger [2].

Feynman's path integral method is a natural way to calculate transition amplitudes. For classically allowed transitions one has to identify all classically allowed trajectories, assign each of them with a phase and an amplitude and sum up their contribution. This procedure yields as an approximation the semiclassical amplitude. In a quantum mechanically exact calculation of the propagator one would have to sum up all paths, including the classically forbidden ones. Semiclassical methods work usually very well because classical trajectories carry the main information needed to calculate the transition amplitude from $\mathbf{r}'$ to $\mathbf{r}$ [13]. In particular, semiclassical methods are accurate and useful when large angular momenta are involved. Typical problems with high–angular wave packets require in an exact quantal calculation a non–trivial summation over many partial waves of the Green function. This problem is avoided in the semiclassical treatment presented here where no summation over partial waves is necessary. For $E < 0$ a particle will move on an ellipse in a plane with the center of force in one focus. The binding energy fixes the length of the semimajor axis while the semiminor axis will also depend on the angular momentum. As shown in Fig. 2, the classically allowed trajectories are confined to the volume in position space defined by the equations of motions for a given initial absolute value of the velocity. In two dimensions, one has a critical ellipse that leads to a finite classical motion.

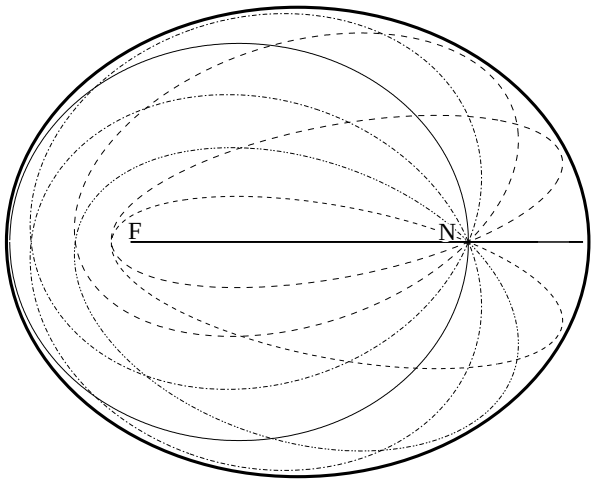

FIG. 2: The caustic (thick solid line) for the Kepler problem is an ellipse. Classically allowed orbits with the same energy, the same center of force F and a common starting point N have to lie inside this critical ellipse.

From the definition (1) of α_+ and α_- it follows that $\alpha_+/2$ and $\alpha_-/2$ are the distances of m and n from point F (see Fig. 1). Hence we identify the distances $\alpha_\pm$ as path coordinates of n and m along the straight line $\overline{Fnm}$ with F as origin. Energy conservation $H = E$ in Eq. (2) yields the velocities

$$v_\pm = \sqrt{\frac{2|E|}{\mu}}\sqrt{\frac{4a-\alpha_\pm}{\alpha\pm}} \tag{13}$$

in m and n. By making use of the coordinates $\alpha/2$ and velocities $v(\alpha)$ we obtain the reduced action for travelling from n to m:

$$W(\mathbf{r},\mathbf{r}';E) = W_+(\alpha_+,E) - W_-(\alpha_-,E)\,, \tag{14}$$

where

$$\begin{aligned} W_\pm &= \mu\int_0^{\alpha_\pm/2} v_+\,\mathrm{d}(\tilde{\alpha}_\pm/2) \\ &= \mu\int_0^{\alpha_\pm/2}\sqrt{\frac{K_c}{\mu a}}\frac{\sqrt{a\tilde{\alpha}_\pm-(\tilde{\alpha}_\pm/2)^2}}{\tilde{\alpha}_\pm/2}\,\mathrm{d}(\tilde{\alpha}_\pm/2) \end{aligned} \tag{15}$$

can be cast in closed form

$$W_\pm = \sqrt{\frac{K_c\mu}{a}}\left(\frac{1}{2}\sqrt{(4a-\alpha_\pm)\alpha_\pm}+2a\arctan\sqrt{\frac{\alpha_\pm}{4a-\alpha_\pm}}\right). \tag{16}$$

The last three equations are consistent with Eqs. (8) and (9) and confirm the essentially one–dimensional character of the reduced action for the Kepler and Coulomb problem.

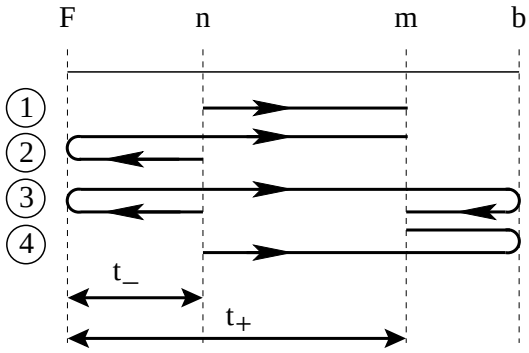

FIG. 3: The four elementary paths from n to m according to Lambert's mapping theorem. The travel time for each path can be expressed by t_- , t_+ and the time for a round trip.

IV. SEMICLASSICAL ENERGY GREEN FUNCTION

The n–dimensional energy Green function is a solution of the inhomogeneous stationary Schrödinger equation

$$[E - H]\, G^{(n)}(\mathbf{r}, \mathbf{r}'; E) = \delta^{(n)}(\mathbf{r} - \mathbf{r}'). \tag{17}$$

with $\delta^{(n)}$ being a delta–function point source in n dimensions. Different boundary conditions on $G^{(n)}$ are possible. For scattering problems, outgoing–wave boundary conditions are usually appropriate. For standing waves and for bound–state problems $G^{(n)}$ is real. $G^{(n)}(\mathbf{r}, \mathbf{r}'; E)$ characterizes the probability-amplitude for traveling from $\mathbf{r}$ to $\mathbf{r}'$ with a given energy E. For the n-dimensional Coulomb problem the Hamiltonian is given by

$$H = -\frac{\hbar^2}{2m}\mathbf{\Delta} + \frac{K_c}{r}\,, \tag{18}$$

where $\mathbf{\Delta}$ is the Laplace operator and r the distance from the force center in n dimensions.
The semiclassical limit of the energy Green function is given by [4, 5, 6, 7]

$$G^{(n)}_{\rm sc}(\mathbf{r}, \mathbf{r}'; E) = \frac{1}{\mathrm{i}\hbar} \sum_i \frac{-1}{(-2\pi\mathrm{i}\hbar)^{(n-1)/2}} \left|\mathbf{D}(W_i(\mathbf{r}, \mathbf{r}'; E))\right|^{1/2} \times \exp\left[\frac{\mathrm{i}}{\hbar} W_i(\mathbf{r}, \mathbf{r}'; E) - \mathrm{i}m_i\frac{\pi}{2}\right], \tag{19}$$

where

$$\mathbf{D}(W(\mathbf{r}, \mathbf{r}'; E)) = \det\begin{pmatrix} \frac{\partial^2 W}{\partial \mathbf{r}\partial \mathbf{r}'} & \frac{\partial^2 W}{\partial \mathbf{r}\partial E} \\ \frac{\partial^2 W}{\partial E \partial \mathbf{r}'} & \frac{\partial^2 W}{\partial E^2} \end{pmatrix} \tag{20}$$

is the Van Vleck–Pauli–Morette (VVPM) determinant. In Eq. (19) one has to sum over all classical fixed–energy paths i leading from $\mathbf{r}'$ to $\mathbf{r}$ and having the reduced action W_i. The VVPM–determinant contains derivatives of second order with respect to $\mathbf{r}$, $\mathbf{r}'$ and E. For example, $\frac{\partial^2 W}{\partial \mathbf{r}\partial \mathbf{r}'}$ is a $n \times n$ matrix with mixed derivatives with respect to starting (initial) and ending (final) points $\mathbf{r}' = (x'_1, x'_2, ..., x'_n)$ and $\mathbf{r} = (x_1, x_2, ..., x_n)$.
Finally, m_i is the Morse index which is the number of conjugate points along the trajectory from $\mathbf{r}' = (x'_1, x'_2, ..., x'_n)$ to $\mathbf{r} = (x_1, x_2, ..., x_n)$. In the next section the indices will be read off from the analytical result for the VVPM–determinant. We have seen before that Lambert's theorem allows the Coulomb problem to be mapped on a 1–D problem. Utilizing Lambert's projection theorem, we are now in a position to find *all* possible trajectories and, if needed, all traveling times. Figure 3 reveals all elementary possibilities to travel from n to m. As in Fig. 1 already mentioned, we regard the motion in 1-D as motion on an ellipse with infinitesimally small semiminor axis b. For such motion we obtain Table I, where

$$W_{2\pi} = 2\pi\sqrt{\mu a K_c} \quad \text{and} \quad T_{2\pi} = 2\pi\sqrt{\frac{\mu a^3}{K_c}} \tag{21}$$

denote the action for a closed orbit and the time of circulation on the same closed orbit respectively. We observe that both quantities depend only on the semimajor axis a, i.e. on the orbital energy E.
Traveling from $\mathbf{r}'$ to $\mathbf{r}$ at constant energy is possible along one of the four elementary paths. However there is an infinite number of possibilities for traveling due to the addition of an arbitrary number of loops to each elementary path.

V. THE VAN VLECK–PAULI–MORETTE DETERMINANT

We will now calculate the amplitude of the Green's function, i.e. the VVPM determinant $\mathbf{D}(W)$ (Eq. 20). It is helpful to realize that the $n\times n$ sub-determinant $\left|\frac{\partial^2 W}{\partial \mathbf{r}\partial \mathbf{r}'}\right|$ vanishes ([4], page 24). Therefore $\mathbf{D}(W)$ is independent of the matrix element $\left|\frac{\partial^2 W}{\partial E^2}\right|$. We will replace this element by 0. The VVPM matrix contains mixed second derivatives of W with respect to the coordinates x'_i and x_j. In the last section we showed how to express the reduced action for the elementary four paths as combinations of the two basic actions $W_+(\alpha_+(\mathbf{r}, \mathbf{r}'))$ and $W_-(\alpha_-(\mathbf{r}, \mathbf{r}'))$ (Fig. 3 and Table I). By using $\frac{\partial W_\pm}{\partial(\alpha_\pm/2)} = \mu v_\pm$ together with the chain rule we find for the off diagonal ($i \neq j$) elements

path	action	travel time	Morse index
① direct path	$W_1 = W_+ - W_-$	$T_1 = t_+ - t_-$	0
② reflection at F	$W_2 = W_+ + W_-$	$T_2 = t_+ + t_-$	1
③ two reflections	$W_3 = W_{2\pi} + (W_+ - W_-)$	$T_3 = T_{2\pi} - (t_+ - t_-)$	2
④ reflection at the caustic	$W_4 = W_{2\pi} - (W_+ + W_-)$	$T_4 = T_{2\pi} - (t_+ + t_-)$	1

TABLE I: Reduced action and Morse-indices m_i for bounded motion along the four elementary trajectories in classically allowed regions for an attractive Coulomb potential in three dimensions (see also Fig. 1). The reduced actions are combinations of W_+ and W_- and the Morse indices in n dimensions are obtained in Sec. V.

$$\frac{\partial^2 W_+}{\partial x_i \partial x'_j} = \frac{\mu}{4}\frac{\partial v_+}{\partial(\alpha_+/2)}\left(\frac{x'_j}{r'} - \frac{x_j - x'_j}{s}\right)\left(\frac{x_i}{r} + \frac{x_i + x'_i}{s}\right) + \frac{\mu v_+}{2}\frac{(x_i - x'_i)(x_j - x'_j)}{s^3}\,, \tag{22}$$

$$\frac{\partial^2 W_-}{\partial x_i \partial x'_j} = \frac{\mu}{4}\frac{\partial v_-}{\partial(\alpha_-/2)}\left(\frac{x'_j}{r'} + \frac{x_j - x'_j}{s}\right)\left(\frac{x_i}{r} - \frac{x_i + x'_i}{s}\right) - \frac{\mu v_-}{2}\frac{(x_i - x'_i)(x_j - x'_j)}{s^3}\,, \tag{23}$$

where we made use of the fact that according to Eq (13) the $v_\pm$ are functions of $\alpha_\pm$. The diagonal elements follow in a similar fashion

$$\frac{\partial^2 W_+}{\partial x_j \partial x'_j} = \frac{\mu}{4}\frac{\partial v_+}{\partial(\alpha_+/2)}\left(\frac{x'_j}{r'} - \frac{x_j - x'_j}{s}\right)\left(\frac{x_j}{r} + \frac{x_j + x'_j}{s}\right) - \frac{\mu v_+}{2s}\left(1 - \frac{(x_j - x'_j)^2}{s^2}\right)\,, \tag{24}$$

$$\frac{\partial^2 W_-}{\partial x_j \partial x'_j} = \frac{\mu}{4}\frac{\partial v_-}{\partial(\alpha_-/2)}\left(\frac{x'_j}{r'} + \frac{x_j - x'_j}{s}\right)\left(\frac{x_j}{r} - \frac{x_j + x'_j}{s}\right) + \frac{\mu v_-}{2s}\left(1 - \frac{(x_j - x'_j)^2}{s^2}\right)\,. \tag{25}$$

The mixed derivatives with respect to energy and coordinates are obtained by utilizing $\frac{\partial W}{\partial E} = t$. We also have $\frac{\partial W_\pm}{\partial E} = t_\pm$. Lambert's projection of the Coulomb problem to a linear, one dimensional motion implies that

$$\frac{\partial^2 W_\pm}{\partial(\alpha_\pm/2)\partial E} = \frac{\partial t_\pm}{\partial(\alpha_\pm/2)} = \frac{\mathrm{d}t_\pm}{\mathrm{d}(\alpha_\pm/2)} = \frac{1}{v_\pm}. \tag{26}$$

We can therefore write

$$\frac{\partial^2 W_+}{\partial x_j \partial E} = \frac{\partial t_+}{\partial(\alpha_+/2)}\frac{\partial(\alpha_+/2)}{\partial x_j} = \frac{1}{v_+}\left(\frac{x_j}{2r} + \frac{x_j - x'_j}{2s}\right)\,, \tag{27}$$

$$\frac{\partial^2 W_-}{\partial x_j \partial E} = \frac{1}{v_-}\left(\frac{x_j}{2r} - \frac{x_j - x'_j}{2s}\right). \tag{28}$$

Finally,

$$\frac{\partial^2 W_+}{\partial x'_i \partial E} = \frac{\partial t_+}{\partial(\alpha_+/2)}\frac{\partial(\alpha_+/2)}{\partial x'_i} = \frac{1}{v_+}\left(\frac{x'_i}{2r'} - \frac{x_i - x'_i}{2s}\right)\,, \tag{29}$$

$$\frac{\partial^2 W_-}{\partial x'_i \partial E} = \frac{1}{v_-}\left(\frac{x'_i}{2r'} + \frac{x_i - x'_i}{2s}\right)\,. \tag{30}$$

In principle it is possible to evaluate the second derivatives for elliptic motion for all points N and M. However this is a tedious task. Fortunately Lambert's theorem tells us that elliptical Kepler motion can be mapped on a degenerate ellipse where motion occurs on a 1–D straight line. We use this mapping and assume the coordinate q to run along this line from $q' = \alpha_-/2$ to $q = \alpha_+/2$, i.e. from point n to point m. In n dimensions we have $n-1$ coordinates $x_2, x_3, \ldots x_n$ that are orthogonal to the trajectory. Along the trajectory we have $x_i = x'_i = 0$ for $i \geq 2$. If we therefore evaluate Eqs. (22)-(30) for $i, j \geq 2$, we observe that the right hand sides vanish except for the diagonal matrix elements

$$\mathcal{F}_+ := \frac{\partial^2 W_+}{\partial x_j \partial x'_j}|_{x_j, x'_j = 0} = -\frac{\mu v_+}{2s}\,, \quad j \geq 2\,, \tag{31}$$

and

$$\mathcal{F}_- := \frac{\partial^2 W_-}{\partial x_j \partial x'_j}|_{x_j, x'_j = 0} = \frac{\mu v_-}{2s}\,, \quad j \geq 2\,. \tag{32}$$

Each direction $i \geq 2$ orthogonal to the straight–line trajectory contributes with the same dimensional factor $\mathcal{F}$. Putting everything together we can cast the

$(n+1)\times(n+1)$ VVPM determinant in a simple form:

$$\mathbf{D}(W)=\det\begin{pmatrix} \frac{\partial^2 W}{\partial(\alpha_+/2)\partial(\alpha_-/2)} & 0 & \cdots & 0 & \frac{\partial^2 W}{\partial(\alpha_+/2)\partial E} \\ 0 & \mathcal{F} & & & 0 \\ \vdots & & \ddots & & \vdots \\ 0 & & & \mathcal{F} & 0 \\ \frac{\partial^2 W}{\partial(\alpha_-/2)\partial E} & 0 & \cdots & 0 & 0 \end{pmatrix}. \tag{33}$$

From Table I we infer that the action W needed for the four elementary paths is always a linear combination of W_+ and W_-. The necessary determinants $\mathbf{D}(W_+\pm W_-)$ are obtained from Eq. (33) with $\mathcal{F}$ replaced by $\mathcal{F}_+\pm\mathcal{F}_-$. Recalling that W_+ (W_-) is a function α_+ (α_-) only, we conclude that

$$\frac{\partial^2 W}{\partial(\alpha_+/2)\partial(\alpha_-/2)}=0. \tag{34}$$

Therefore the entry on the top left of VVPM–matrix vanishes. The determinant is now easily calculated via Laplace expansion. The result is

$$\mathbf{D}(W)=-\frac{\partial^2 W}{\partial(\alpha_+/2)\partial E}\frac{\partial^2 W}{\partial(\alpha_-/2)\partial E}\times\mathcal{F}^{(n-1)}. \tag{35}$$

A straightforward evaluation of Eq. (35) yields simple results for the determinants of the four elementary paths:

$$\begin{aligned}\mathbf{D}①&=\mathbf{D}(W_+-W_-)=\frac{1}{v_+v_-}\left[-\frac{\mu}{2s}(v_++v_-)\right]^{(n-1)}\\ &=-\mathbf{D}③\,,\end{aligned} \tag{36}$$

$$\begin{aligned}\mathbf{D}②&=\mathbf{D}(W_++W_-)=-\frac{1}{v_+v_-}\left[-\frac{\mu}{2s}(v_+-v_-)\right]^{(n-1)}\\ &=-\mathbf{D}④\,.\end{aligned} \tag{37}$$

We should point out that Eq. (35) is also valid for scattering states if action and velocities are adapted to unbounded motion.

We now determine the *Morse indices* m_i which are given by the order of the zeros of the determinants $\mathbf{D}①$ along path number i. Here we restrict ourselves to the three–dimensional Coulomb problem, $n=3$. By inspecting Fig. 3 we see that on path ① the velocities are different from zero because we have assumed that neither point m nor point n is lying on the caustic b. Hence we have $m_1=0$. On path ④ the velocity vanishes at the reflection point b. There a pole of first order is generated in the determinant. As a result we have $m_4=1$, independent of n. Path ② corresponds to elliptic motion with infinitesimally small semiminor axis b with the particle (planet or electron) moving around F with infinite velocity, $v\to\infty$. Along this path it therefore encounters a pole of order $n-2=1$ at F, meaning that the particle picks up the Morse index $m_2=1$. Obviously we have $m_3=m_2+m_4=2$. Finally by inspecting Eq. (36) we observe that a full round trip picks up an additional phase which originates from closing the loop with $v_+=v_-$ and $s=0$, giving rise to a pole of order $n-1=2$ in the determinant. In other words, closed orbits pick the phase $m_{2\pi}=2(n-1)$.

VI. $E<0$: THE BOUND–STATE GREEN FUNCTION

Having found the amplitudes, reduced actions and the correct phases we are in a position to evaluate the semiclassical Green function in analytic form. We showed before that $G_{\rm sc}^{(n)}(\mathbf{r},\mathbf{r}';E)$ consists of the amplitudes for the four elementary trajectories plus a summation over all possible loops for each elementary path. Therefore we can write

$$\begin{aligned}G_{\rm sc}^{(n)}(\mathbf{r},\mathbf{r}';E)=&\frac{1}{\mathrm{i}\hbar}\frac{-1}{(-2\pi\mathrm{i}\hbar)^{(n-1)/2}}\sum_{i=1}^{4}\sum_{j=0}^{\infty}\sqrt{|\mathbf{D}(W_i(\mathbf{r},\mathbf{r}';E)+j\,W_{2\pi}(E))|}\\ &\times\exp\left[\frac{\mathrm{i}}{\hbar}(W_i(\mathbf{r},\mathbf{r}';E)+j\,W_{2\pi}(E))-\mathrm{i}\frac{\pi}{2}(m_i+j\,m_{2\pi})\right]\\ =&G_{\rm elem}(\mathbf{r},\mathbf{r}';E)\times P_{\rm glob}(W_{2\pi},n).\end{aligned} \tag{38}$$

as a product of the elementary four-path Green function $G_{\rm elem}(\mathbf{r},\mathbf{r}';E)$ and and a factor $P_{\rm glob}(W_{2\pi},n)=\sum_{j=0}^{\infty}\exp\left[\mathrm{i}j\left(\frac{W_{2\pi}}{\hbar}-\frac{\pi}{2}m_{2\pi}\right)\right]$ which accounts for the loop summation. The factorization is possible because $\mathbf{D}(W_i(\mathbf{r},\mathbf{r}';E)+j\,W_{2\pi}(E))$ is independent of $W_{2\pi}(E)$. Each loop adds the same non–negative phase to the Green function. The summation over the infinite number

of loops can be carried out. We obtain

$$\sum_{j=0}^{\infty} \exp\left[2\pi \mathrm{i} j \left(\frac{W_{2\pi}}{2\pi\hbar} - \frac{m_{2\pi}}{4}\right)\right] = \frac{1}{2} + \frac{\mathrm{i}}{2} \cot\left[\pi\left(\frac{W_{2\pi}}{2\pi\hbar} - \frac{m_{2\pi}}{4}\right)\right]. \quad (39)$$

The poles of $P_{\mathrm{glob}}(W_{2\pi}, n)$ yield the energy eigenvalues of the hydrogen atom. Obviously, they are obtained from the poles of the cotangent given by the non–negative integers, $\frac{W_{2\pi}}{2\pi\hbar} - \frac{m_{2\pi}}{4} = 0, 1, 2, ...$ Using Eq. (21) together with $m_{2\pi} = 2(n-1)$, it is now easy to extract the exact energy eigenvalues for the hydrogen atom in $n > 1$ dimensions [14]

$$E_k = -\frac{\mu K_c^2}{2\hbar^2} \frac{1}{(k + (n-1)/2)^2} \qquad [k = 0, 1, 2, ...]. \quad (40)$$

We should point out that the correct quantization rule for the action in n dimensions

$$W_{2\pi} = h(k + \frac{n-1}{2}) \qquad [k = 0, 1, 2, ...] \quad (41)$$

is an integer multiple of h only for odd values of n.
The elementary four–path Green function G_{elem} can be written in a more compact fashion because paths lying on the same ellipse have the same amplitude as can be seen from Fig. 1, and Fig. 3. Their Morse indices are related to each other through $m_j = (n-1) - m_i$. Therefore we can merge paths ① and ③ and paths ② and ④ pairwise together. Then the elementary four–path Green function shows a two-path interference pattern.
Putting everything together, we recast the (real) negative energy Green function (38) in the form

$$G_{\mathrm{sc}}^{(n)}(\mathbf{r}, \mathbf{r}'; E) = \frac{1}{\hbar(-2\pi\hbar)^{(n-1)/2}} \frac{1}{\sin(k\pi)} \times \left(\sqrt{|\mathbf{D}\,①\,|}\cos\left[\frac{W_1}{\hbar} - \pi\left(\frac{n-1}{4} + k\right)\right] + \sqrt{|\mathbf{D}\,②\,|}\sin\left[\pi\left(\frac{3(n-1)}{4} + k\right) - \frac{W_2}{\hbar}\right]\right). \quad (42)$$

The bound states (40) at $k = 0, 1, 2, 3, \ldots$ give rise to poles in $G_{\mathrm{sc}}^{(n)}$. Note that in Eq. (42) k can assume any continuous value $k \geq 0$. $\mathbf{D}$① and $\mathbf{D}$② are the Van Vleck–Pauli–Morette determinants given before in Eqs. (36) and (37). The actions $W_1 = W_+ - W_-$ and $W_2 = W_+ + W_-$ are readily calculated from Eq. (16). Equation (42) is the main result of the paper. In the next section we compare the semiclassical result for the Green function with the exact quantum result. The case $E > 0$ will be treated in App. B.

VII. RESULTS AND COMPARISON WITH THE EXACT PROPAGATOR

In a last step we compare the analytic expressions for the Coulomb Green function with the exact quantum mechanical Green function as a function of $\mathbf{r}$. We use atomic units. Fig. 4 shows contour plots of the three dimensional Green function $G(\mathbf{r}, \mathbf{r}'; E)$. In order to avoid the infinities at integer principal quantum numbers, we have chosen the non–integer 'principal' quantum number $\nu = k+1 = 29.2$ in Eq. (40). This value is close to the one treated numerically in [10]. The center of force is located at the origin, the starting point with $\mathbf{r}' = (1232, 0, 0)$ Bohr radii has been chosen to lie on the x axis. The end point $\mathbf{r}$ is varied in the x, y- plane.
To illustrate the meaning of G we assume to have a coherent stationary source $\sigma(\mathbf{r}')$ of independent particles. Such a source will generate the following wave function:

$$\psi(\mathbf{r}, E) = \int G(\mathbf{r}, \mathbf{r}'; E)\, \sigma(\mathbf{r}')\, \mathrm{d}\mathbf{r}'. \quad (43)$$

For a point like source at $\mathbf{r}'$ the plot of the Green function reveals how particles leak out of the point source at $\mathbf{r}'$ under the influence of the Coulomb field. In our case G is real; hence there is no net current flowing out of the source. All particles are eventually reflected back into

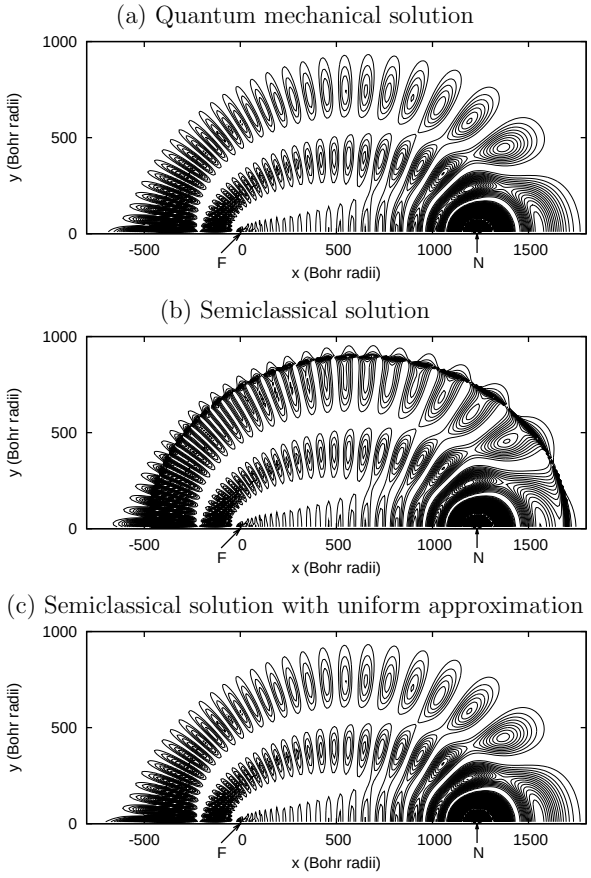

FIG. 4: Contour plot of $|G^{(3)}(\mathbf{r}, \mathbf{r}'; E)|^2$ with 'principal' quantum number $\nu = 29.2$ and center of force F at the origin. The initial position vector N at $\mathbf{r}' = (1232, 0, 0)$ Bohr radii is located on the x axis, the final position vector $\mathbf{r}$ is varied in the x, y-plane.

the source. A comparison with the exact Green function shows that all features, including the nodal structure are mirrored perfectly by the semiclassical Green function. However we must face the fact that the semiclassical approach will fail at the caustic where two trajectories merge into one. Here the deficiency can be repaired by making use of the uniform approximation (see App. C). The uniform approximation is slightly more complex than the semiclassical approximation.

To demonstrate how well the approximation works we present a cut of the Green function parallel to the x–axis (Fig. 5). The semiclassical approximation starts to deviate from the exact solution near the caustic where the saddle point approximation that underlies the semiclassical theory is no longer valid. The spike in the figure marks the position of the caustic. At the caustic the semiclassical approximation should be replaced by the uniform approximation which is seen to match the exact quantum solution very well.

The mapping of the Coulomb problem to a 1-D–problem has the great advantage that *tunneling* properties in a Coulomb field can be easily calculated in semiclassical approximation because one can avoid the inherent difficulties associated with multidimensional tunneling. Tunneling trajectories are shown in Fig. 7. In the tunneling region there is exponential decay but no reflection. The analytic continuation of the action into the tunneling sector is given in Appendix C. The same projection method as before can be used. This time the Morse indices are no longer integers and will depend on how deep the particle will move into the tunnel.

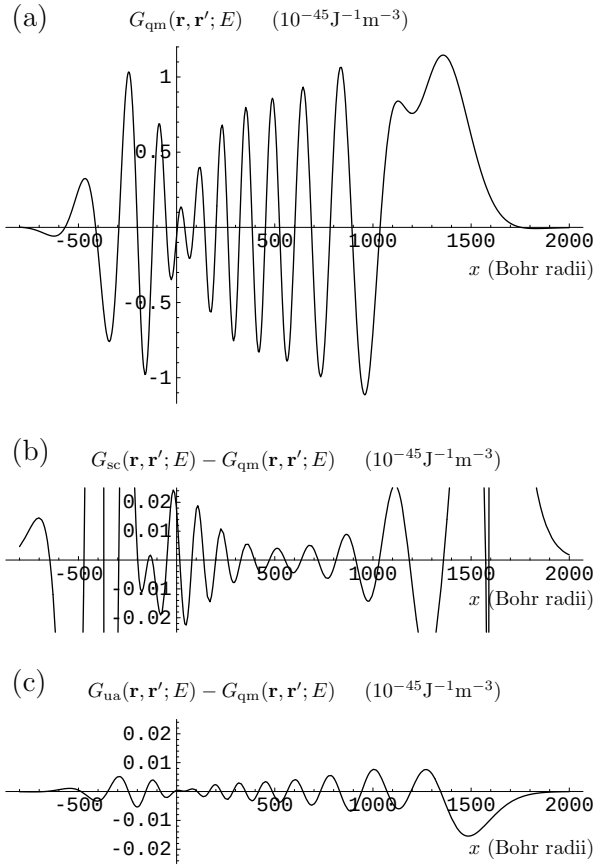

FIG. 5: Plot of $G^{(3)}(\mathbf{r},\mathbf{r}';E)$ with principal quantum number $\nu = 29.2$ and center of force at the origin. The initial position vector is located at $\mathbf{r}' = (1232, 0, 0)$ Bohr radii, the final position vector shown along the x-axis for fixed $y = 400$ Bohr radii. (a) Quantum mechanical Green function, (b) deviation of the semiclassical Green function from the quantum mechanical one, (c) deviation of the uniformly approximated Green function from the quantum mechanical result. The uniform approximation agrees with the quantum mechanical result better than 1/100.

VIII. CONCLUDING REMARKS

Lambert's theorem has proven powerful for calculating the semiclassical Green function (Eq. (42)) because it allows to parameterize all dynamical quantities in terms of distances. This feature allowed us to eliminate the eccentric anomaly which is ambiguous in the angles and therefore has to be treated very carefully [15]. The n-dimensional Coulomb problem could be reduced to one dimensional motion. The reduction is achieved by the introduction of new variables $\alpha_\pm = r + r' \pm s$. All necessary reduced actions could then be found analytically. We derived a closed expression for the semiclassical Green function. The Morse indices followed directly from the analytic form of the Van Vleck–Pauli–Morette determinant.

The semiclassical energy Green function is found to be an excellent approximation to the exact Green function. It also yields the correct bound–state energies for hydrogen in all dimensions. We should point out that the semiclassical approximation also works very reliably even at low energies with small principal quantum numbers. We found that also in those cases semiclassics matches the quantum mechanical Green function extremely well. For small quantum numbers one has less nodes and the elliptically shaped caustic shrinks.

In energetically forbidden regions there are no classical trajectories. Nevertheless we can continue the semiclassical Green function into the tunnel. The exit of the tunnel can be dealt with in semiclassics by invoking corrections given by the uniform approximation.

The motion in a Coulomb potential is an important problem in quantum mechanics. It is therefore useful to learn how the semiclassical limit of the energy Coulomb Green function emerges from a coherent summation of all amplitudes that belong to an infinite number of classical trajectories. The results of this paper can be readily implemented into real–space problems in the presence of Coulomb interaction. One example is the quantum behavior of Rydberg atoms [10, 16].

Acknowledgments

This work was supported by DFG grant KL 315/7–1 and the Emmy-Noether program of the DFG (grant KR 2889/2-1). We appreciate helpful discussions with Eric J. Heller, Erich Mueller, and Jan M. Rost.

APPENDIX A: REDUCED COULOMB ACTION

In order to eliminate the eccentricity ϵ in Eq. (14) in favor of spatial positions we introduce in a first step the new variables

$$\cos g := \epsilon \cos\left(\frac{\xi+\xi'}{2}\right) \quad \text{and} \quad d := \frac{\xi-\xi'}{2}\,. \tag{A1}$$

In a second step we substitute

$$\gamma := d+g \quad \text{and} \quad \delta := g-d \tag{A2}$$

to arrive at Eq. (8). We next relate the variables γ and δ to spatial positions. The radial position of any point M or N on the ellipse (see Fig. 1) relative to the center of force is given by

$$r^2 = [(x-\epsilon a)^2 + y^2], \tag{A3}$$

where x and y are the coordinates relative to the center of the ellipse. With the help of Eq. (5) we easily find

$$r = a(1-\epsilon\cos\xi) \tag{A4}$$

In terms of the variables g and d we have

$$r + r' = 2a(1-\cos g\cos d) \tag{A5}$$

and

$$|\mathbf{r}-\mathbf{r}'| = 2a|\sin d\cos g| \tag{A6}$$

Without loss of generality we can assume $0 \le d \le \pi$ and $0 \le g \le \pi/2$. From the last two equations we then readily confirm the desired result, Eq. (9).

APPENDIX B: $E > 0$: SCATTERING STATES

To treat scattering states in semiclassical approximation we can use the same formalism as for bound states. In an attractive force field and for $E > 0$, there is no caustic and hence no reflection at b. As can be seen from Fig. 6 we then have only two hyperbolic trajectories leading from N to M. The one–dimensional variables are again $\alpha_\pm = r + r' \pm |\mathbf{r}-\mathbf{r}'|$. The projection of the motion onto a line applies again but we have to consider the change in geometry.

1. Attractive Coulomb Interaction

In this case we obtain

$$\begin{aligned} G^{(n)}_{\mathrm{sc,attr}}(\mathbf{r},\mathbf{r}';E) &= -\frac{\mathrm{i}}{\hbar}\frac{1}{(2\pi\mathrm{i}\hbar)^{(n-1)/2}} \\ &\times\left(\sqrt{|\mathbf{D}\,①\,|}\exp[\frac{\mathrm{i}}{\hbar}W_1] + \sqrt{|\mathbf{D}\,②\,|}\exp[\frac{\mathrm{i}}{\hbar}W_2 - \mathrm{i}\frac{\pi}{2}(n-2)]\right), \end{aligned} \tag{B1}$$

with $W_1 = W_+ - W_-$ and $W_2 = W_+ + W_-$. The action follows again from Eq. (16), adapted to $E > 0$,

$$\begin{aligned} (W_\pm)^{(E>0)}_{\mathrm{attr}} &= \mu\sqrt{\frac{K_c}{\mu a}}\int_{2a}^{\alpha_\pm/2}\sqrt{\frac{2a+\tilde\alpha_\pm/2}{\tilde\alpha_\pm/2}}\,\mathrm{d}(\tilde\alpha_\pm/2) \\ &= \sqrt{\frac{K_c\mu}{a}}\left(\frac{1}{2}\sqrt{(4a+\alpha_\pm)\alpha_\pm} + 2a\log\frac{\sqrt{\alpha_\pm}+\sqrt{4a+\alpha_\pm}}{\sqrt{4a}}\right). \end{aligned} \tag{B2}$$

2. Repulsive Coulomb Interaction

If the potential is repelling we have again two hyperbolic trajectories which connect N and M. But now a caustic separates the classically allowed region from the energetically forbidden region. Classically allowed motion occurs for $4|a| < \alpha_\pm$. The corresponding reduced action reads

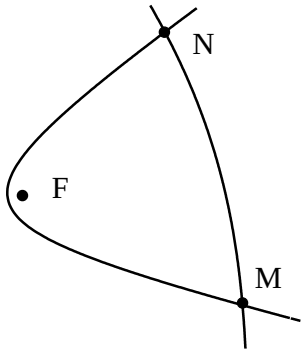

FIG. 6: For $E > 0$, hyperbolic trajectories connect N and M, with the center of force at F. In the repulsive case (not shown) there is a caustic in contrast to the attractive case where every point in space can be reached.

$$\begin{aligned}(W_\pm)_{\rm rep}^{(E>0)} &= \mu\sqrt{\frac{K_c}{\mu|a|}}\int_{2a}^{\alpha_\pm/2}\sqrt{\frac{-2|a|+\tilde\alpha_\pm/2}{\tilde\alpha_\pm/2}}\,{\rm d}(\tilde\alpha_\pm/2)\\ &= \sqrt{\frac{K_c\mu}{|a|}}\left(\frac{1}{2}\sqrt{(-4|a|+\alpha_\pm)\alpha_\pm}+|a|\log\frac{\sqrt{\alpha_\pm}-\sqrt{-4|a|+\alpha_\pm}}{\sqrt{\alpha_\pm}+\sqrt{-4|a|+\alpha_\pm}}\right).\end{aligned} \tag{B3}$$

For completeness we write down the action in the classically forbidden tunneling region where $\alpha_- < 4|a|$:

$$\begin{aligned}(W_-)_{\rm rep}^{(E>0)} &= \pm{\rm i}\mu\sqrt{\frac{K_c}{\mu|a|}}\int_{2a}^{\alpha_-/2}\sqrt{\frac{2|a|-\tilde\alpha_-/2}{\tilde\alpha_-/2}}\,{\rm d}(\tilde\alpha_-/2)\\ &= \pm{\rm i}\sqrt{\frac{K_c\mu}{|a|}}\left(-\pi|a|+\frac{1}{2}\sqrt{(4|a|-\alpha_-)\alpha_-}+2|a|\arctan\sqrt{\frac{\alpha_-}{4|a|-\alpha_-}}\right).\end{aligned} \tag{B4}$$

APPENDIX C: ANALYTIC CONTINUATION INTO THE TUNNELING REGION

1. Uniform Approximation

The semiclassical Green function is derived from the exact expression for the quantum mechanical Green function by making use of the saddle point approximation (SPA). However this approximation is not valid at the caustic where two saddle points merge into one. In this case the uniform approximation (UA) will cure the deficiency of the SPA. The method is standard. For more details the reader is referred to [5], p. 118ff, p. 131ff. Here we follow the method outlined in reference [17]. For $n = 3$ we have

$$G_{\rm ua}(\mathbf{r},\mathbf{r}';E) = \frac{{\rm e}^{{\rm i}\xi}}{2\hbar^2\sqrt{\pi}}\left(d_0{\rm Ai}(-\zeta)-{\rm i}d_1{\rm Ai}'(-\zeta)\right) \tag{C1}$$

with

$$\xi = \begin{cases}\frac{1}{2\hbar}\,(W_+ + W_-) & \text{if } \Im(W_-)=0,\\ \Re(W_+/\hbar) & \text{if } \Im(W_-) = -\Im(W_+),\end{cases} \tag{C2}$$

$$\zeta = \begin{cases}\left[\frac{3}{4\hbar}\,(W_+ - W_-)\right]^{2/3} & \text{if } \Im(W_-)=0,\\ -\frac{3}{2}[\Re(W_+/\hbar)]^{2/3} & \text{if } \Im(W_-) = -\Im(W_+),\end{cases} \tag{C3}$$

and

$$\begin{aligned}d_0 &= \zeta^{1/4}\left[\sqrt{\mathbf{D}(W_+)}+\sqrt{-\mathbf{D}(W_-)}\right]{\rm e}^{-5{\rm i}\pi/4}\\ d_1 &= \zeta^{-1/4}\left[\sqrt{\mathbf{D}(W_+)}-\sqrt{-\mathbf{D}(W_-)}\right]{\rm e}^{-5{\rm i}\pi/4}.\end{aligned} \tag{C4}$$

2. Tunneling Regime

Here we look at classically forbidden motion $\alpha_+ > 4a$. This means that point m is lying in the tunnel (see Fig. 7). Whereas W_- is not changed, W_+ must be continued into the classically forbidden space sector. The analytic continuation is obtained by making use of Eq. (16)

$$
\begin{aligned}
(W_+)_{\text{forb}} &= \mu\sqrt{\frac{K_c}{\mu a}}\left(\int_0^{2a}\sqrt{\frac{2a-\tilde{\alpha}_\pm/2}{\tilde{\alpha}_\pm/2}}\,\mathrm{d}(\tilde{\alpha}_\pm/2) \pm \mathrm{i}\int_{2a}^{\alpha_\pm/2}\sqrt{\frac{-2a+\tilde{\alpha}_\pm/2}{\tilde{\alpha}_\pm/2}}\,\mathrm{d}(\tilde{\alpha}_\pm/2)\right) \\
&= \sqrt{\frac{K_c\mu}{a}}\left(a\pi \pm \mathrm{i}\left(\frac{1}{2}\sqrt{(-4a+\alpha_\pm)\alpha_\pm} + 2a\log\frac{\sqrt{4a}}{\sqrt{\alpha_\pm}+\sqrt{-4a+\alpha_\pm}}\right)\right)
\end{aligned}
\tag{C5}
$$

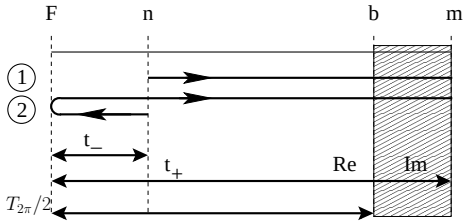

FIG. 7: Bound states and tunneling trajectories: We use the projection formalism to find two possible paths to a point in the classically forbidden region. As the electron passes through b into the tunneling space sector, action and velocity become complex (see Eq. (C5)).

There are two complex conjugated solutions. For the propagator we select the term with positive imaginary part to ensure that the wave function decays exponentially deep in the tunnel. Note however that both solutions will contribute to the uniform approximation in the vicinity of the tunnel exit.

[1] L. Hostler and R. Pratt, Phys. Rev. Lett. **10**, 469 (1964).
[2] J. Schwinger, J. Math. Phys. **5**, 1606 (1964).
[3] M. Gutzwiller, J. Math. Phys. **8**, 1979 (1967).
[4] M. Gutzwiller, *Chaos in classical and quantum mechanics* (Springer, New York, 1990).
[5] L. Schulman, *Techniques and Applications of Path Integration* (Wiley, New York, 1981).
[6] H. Kleinert, *Path Integrals in Quantum Mechanics, Statistics and Polymer Physics* (World Scientific, Singapore, 1990).
[7] C. Grosche and F. Steiner, *Handbook of Feynman Path Integrals*, vol. 145 of *Springer Tracts in Modern Physics* (Springer, Berlin, 1998).
[8] E. Kelsey and J. Macek, J. Math. Phys. **17**, 1182 (1976).
[9] W. Dittrich and M. Reuter, Am. J. Phys. **67**, 768 (1999).
[10] B. Granger, E. Hamilton, and C. Greene, Phys. Rev. A **64**, 042508 (2001).
[11] J. Lambert, *Insigniores orbitae Cometarum proprietates* (Klett, Augsburg, 1761), online: http://num-scd-ulp.u-strasbg.fr:8080/107/.
[12] L. Hostler, J. Math. Phys. **5**, 591 (1963).
[13] M. Brack and R. Bhaduri, *Semiclassical Physics* (Addison-Wesley, Reading, MA, 1997).
[14] M. M. Nieto, Am. J. Phys. **47**, 1067 (1979).
[15] H. Plummer, Royal Astronomical Society **69**, 181 (1909).
[16] C. Ates, A. Eisfeld, and J. M. Rost, New Journal of Physics **10**, 045030 (2008).
[17] D. Richards, *Advanced Mathematical Methods with Maple* (Cambridge University Press, Cambridge, 2002).